In: AIAA SciTech 2023 Forum, 23-27 January, National Harbor, Maryland, USA
DOI:10.2514/6.2023-1082

A TEG-Excited Switched Reluctance Generator for Self-Powered Sensing in Next Generation Aircraft

B. Zaghari*
Centre for Propulsion and Thermal Power Engineering, Cranfield University, Cranfield, Bedfordshire, MK43 0AL, UK

A. Stuikys†
RETORQ Motors Ltd., London, N1 7GU, UK

A S. Weddell‡, N. Grabham§, and N M. White¶
School of Electronics and Computer Science, University of Southampton, Southampton, SO17 1BJ, UK

T J. Harvey‖ and L. Wang**
National Centre for Advanced Tribology at Southampton (nCATS), University of Southampton, Southampton, SO17 1BJ, UK

New aircraft concepts are proposed to support emission reduction in aviation. To achieve the advantages of these concepts an electrical system with high power delivery and low system mass needs to be considered. The reduction of weight of all sub-components without compromising on reliability is being investigated. To achieve these self-powered systems can be introduced to monitor safety critical components. Locally embedded wireless self-powered systems can reduce the weight associated with health monitoring significantly compared to wired systems. In this paper a self-powered system that can be embedded in the engine is introduced. Switched reluctance generator integrated with a thermoelectric generator (TEG) is designed to provide power for bearing health monitoring. An efficient switched reluctance generator is designed for the limited amount of space in the aircraft engine. Two configurations for a six stator poles and fifteen rotor poles (6/15), three phase switched reluctance generator were compared and highest power output was obtained when the individual phase coils were connected in parallel. To achieve efficient energy conversion, the design process and selection of the excitation and generation angles played an important role.

I. Introduction

The electrified aircraft concept is leading to an increase in onboard electrical components to provide power, actuation, and control for aircraft subsystems that have conventionally been powered by other means. As the number of electrical components increases in the aircraft, the need for failure assessment and health monitoring of electrical and mechanical components increases too. The sensors and their processing systems that are embedded for health or performance monitoring require power to function. Self-powered systems are proposed when enough energy cannot be sustained by batteries or supercapacitors for a long-term operation. In the case of electrified aircraft there will be several mechanical

*Lecturer in Propulsion Integration and AIAA member
†Director
‡Lecturer
§Senior Research Fellow
¶Professor
‖Senior Research Fellow
**Professor of Tribo-Sensing

and electrical systems that will require health monitoring and depending on their location the energy required for sensing, data acquisition, and data transmission can be provided by the main energy storage or generators that are connected to the gas turbines. However, there is still a need for an integrated self-powered system so that the energy source and the sensors are in close proximity. Such closely integrated self-powered systems hold great potential for substantial reduction or complete elimination of cabling and their associated system faults. In this paper we are proposing a self-powered sensing system designed for bearing health monitoring. However, the concept of energy harvesting and smart sensing can be applied to the other critical components in the engine or landing gears in more/all electric aircraft.

In previous studies we investigated a wireless smart bearing with embedded accelerometers, thermocouples, and strain gauges integrated in an engine to enable bearing condition monitoring [1]. The challenges of integrating wireless smart sensing systems are: providing enough power for online processing, data acquisition, and wireless transmission; high temperature for sensors and electrical components; limited space and restrictions in sizing of the components. In our previous study we evaluated the energy harvested by thermoelectric generators (TEGs) as the main source of energy [1]. Other methods of energy harvesting for aircraft condition health monitoring is summarised in [2].

In this paper we are presenting an efficient Switched Reluctance Generator (SRG) when the excitation power is provided by the TEGs to facilitate excitation action for the power generation process. The smart sensing system that is integrated in the engine has to operate at high temperature and in a limited space without a dedicated cooling mechanism. Both thermoelectric generators and the switched reluctance machine are selected since they can be designed to operate in harsh environments at high temperature. They also do not interfere with the lubrication of the bearings. SRG could be turned off intermittently to reduce the magnetic field, that can trap conductive particles, when they need to be taken away from the bearings during lubrications. Due to these key advantages the SRG is chosen even though it has lower power density in comparison with permanent magnet machines.

Switched Reluctance Motors (SRM) and generators have been studied for more and all electric aircraft [3] due to their advantages of supply chain security and sustainability. In 1995 a 30kW SRG/SRM with rotational speed of 52krpm and 270Vdc was proposed for stating a turbine engine and extracting power from the engine [4]. This machine was designed to operate from -51 to +125°C. The SRM was tested at 20.8kW and 31krpm and was 88% efficient. However, the performance of SRGs when the input voltage and stack length is very limited has not been explored in previous studies. Significantly lower DC-bus voltage and generator excitation current is considered in this paper in comparison with other SRG applications in aerospace [5] or other applications [6]. This paper shows two design strategies based on the phase coil configurations that lead to higher efficiency.

A. Self-powered system design

The switched reluctance generator considered in this study is designed to be embedded in the engine as shown in Fig. 1. The TEGs and the location of smart bearing is also identified. Greater temperature variation is ideal for thermoelectric energy harvesters, hence a location close to the selected bearing was considered. Two TEGs with reverse modules were considered. TEG1 uses the lower temperature oil and the hot side is attached close to the bearing and TEG2 uses higher temperature oil and attached to a colder surface. In this way temperature difference was provided for the TEGs. Engine oil used for bearing lubrication was used to cool down TEG1 and heat up the second one. The testing results and the architecture of smart sensing including the sensors, energy harvesting from the TEGs, and wireless transmission was presented in [1]. We demonstrated that under a simulated engine environment, the thermoelectric generator can provide sufficient energy for a wireless sensing system to collect environmental data every 46 s, and transmit every 260 s, during the critical take-off phase of flight and part of cruise [1]. However, if more data needs to be collected and transmission occurrences need to be reduced, more power is required. Hence, we are suggesting a switched reluctance generator that is integrated on the shaft near the bearing and converts part of the engine mechanical power to electrical power.

Switched reluctance generators require electrical excitation input power to generate output power. In this study it is assumed that the input power is provided by the TEG and then stored in a capacitor and then used as an excitation source for the SRG. The diagram in Fig. 2 show TEG and SRG connected together to provide necessary power for sensing and wireless data transmission. To prevent the TEG to act as an energy sink a diode is connected to the converter to prevent current flowing back to the TEG.

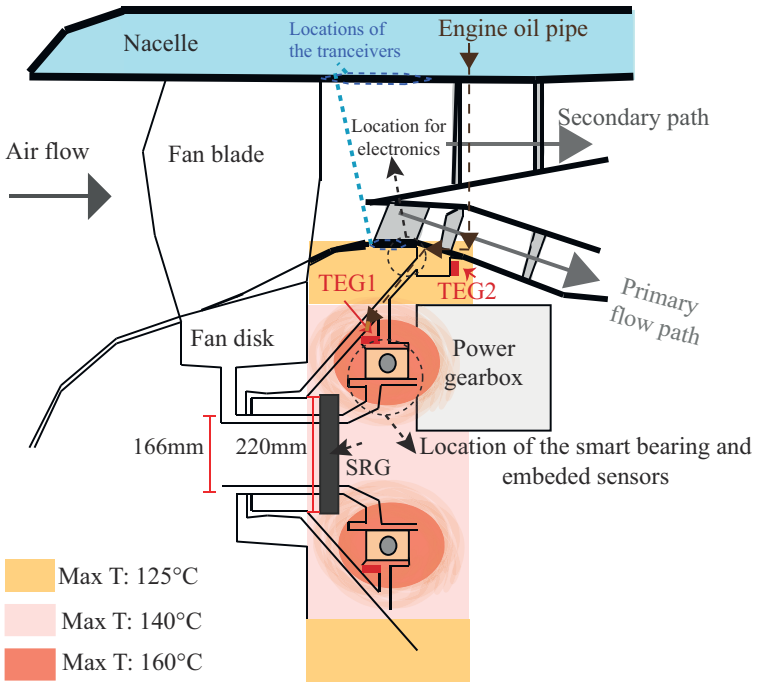

Fig. 1 SRG and the smart bearing integrated in the engine. Schematic cross-section of the engine is provided by Safran Aircraft Engine.

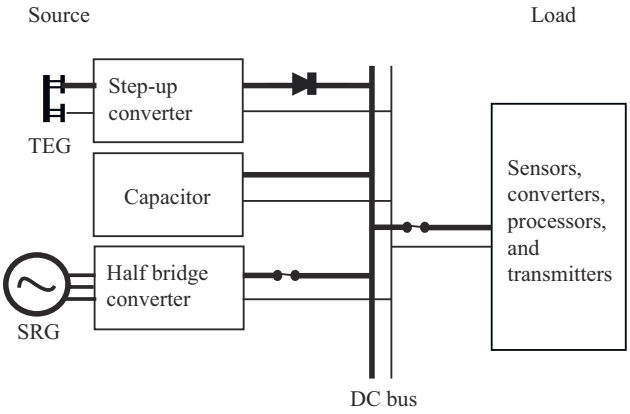

Fig. 2 Diagram showing TEG, SRG, and ultracapacitors as energy sources and sensors, processing, and transmission components as loads

II. Switched reluctance generator design

The switched reluctance generator was designed based on the design restrictions assigned by Safran Engine due to the space availability and close proximity to the bearing that needs to be monitored. The geometry and phase configuration of the proposed SRG is shown in Fig. 3 and the design parameters are presented in Table 1.

Design parameters	Values
Stack length [mm]	50
Air gap length [mm]	1
Iron core material	M35
Wire diameter [mm]	0.5
Number of turns per coil	100
Internal resistance for coils in series (R) [Ohm]	1.4
Internal resistance for coils in parallel (R) [Ohm]	0.35
Slot fill factor [%]	50
Stator pole arc (β_s) [degrees]	4
Rotor pole arc (β_r) [degrees]	4
Stator pole pitch [degrees]	24
Rotor pole pitch [degrees]	24
Storage capacitor (C) [F]	0.001
DC-bus input voltage (V_{in}) [V]	5
Input current at source (I_{in}) [A]	1

Table 1 6/15 three phase SRG parameters

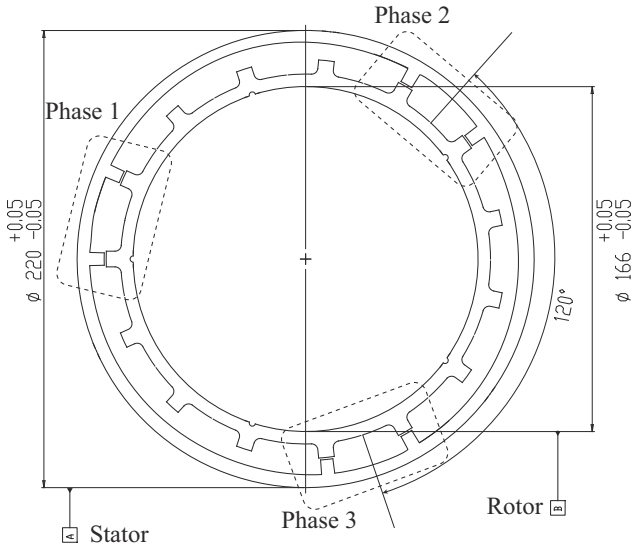

Fig. 3 Front view of a proposed 6/15 three phase SRG.

Symmetric half bridge converter is employed to operate the SRG (Fig. 4). Each converter phase consists of two MOSFETS (IRF7807VPbF) and two diodes (RSX501LAM20) to allow energy recovery to the capacitor C in Fig. 4. Its capacitance must be large enough to maintain the DC-link voltage constant and with low ripple but small enough to be charged quickly after connecting a DC source to the converter. The DC source is the voltage output of the power management system connected to a TEG. The energy source V_{in} charges the capacitor, and after the initial charge, when the required voltage level is established, the source is no longer required. Phase switches in Fig. 4 are on during the magnetizing period, each phase receives the excitation voltage and the current flows through all three phase windings simultaneously. During the excitation period the corresponding phase is energised and during the generation period, the energy flows to the load and or to the storage capacitor, which results in electromechanical energy conversion. The phase switching angles for excitation and generation are selected carefully. The turn-on angle (θ_{on}) is the rotor angle

in which the excitation starts and (θ_{comm}) is the angle where the generation starts, and at (θ_{off}) the generation ends as shown in Fig. 5 .

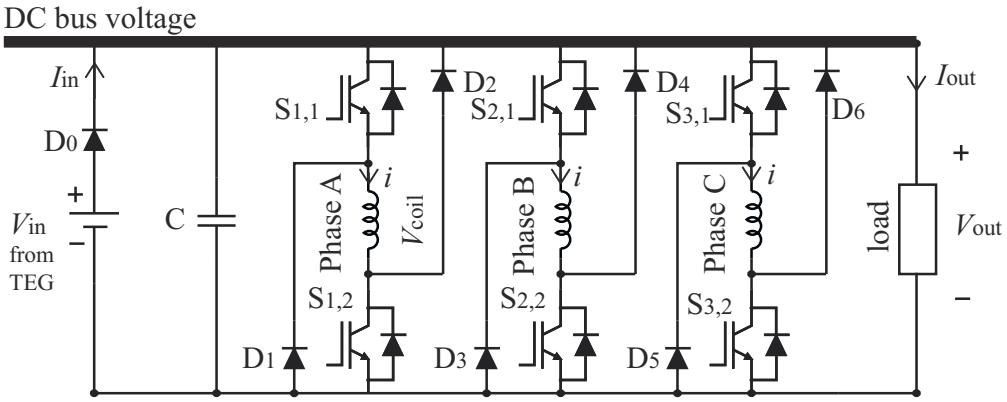

Fig. 4 Half bridge converter circuit diagram for a three phase SRG.

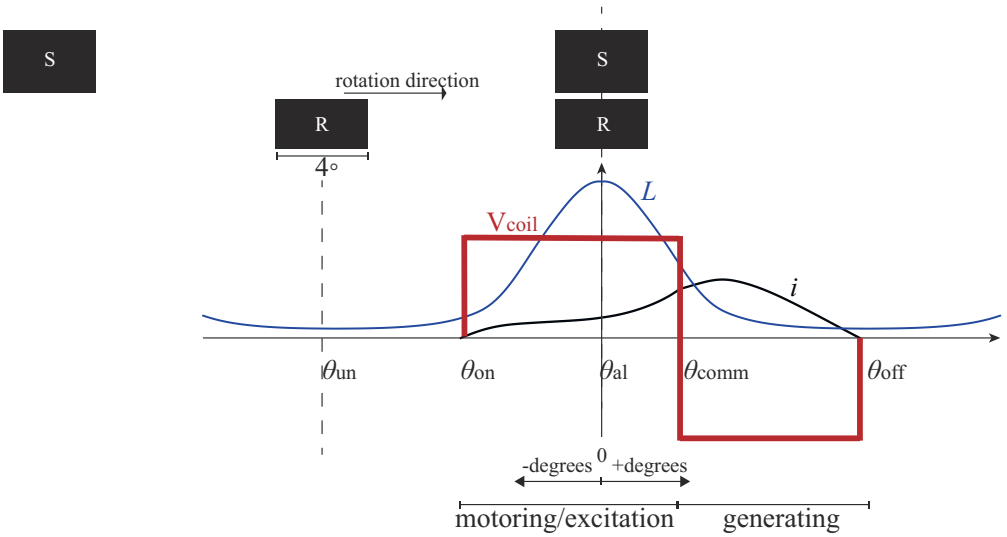

Fig. 5 This diagram presents the voltage and current at different angles, unaligned angle θ_{un}, turn on angle θ_{on}, aligned angle θ_{al}, commutation angle θ_{comm}, and turn off angle θ_{off}.

A switched reluctance machine operates in a generating mode if each phase is excited when the phase inductance is decreasing, $\frac{\mathrm{d}L}{\mathrm{d}\theta} < 0$. The electrical dynamics of an SRG without considering the saturation is

$$V_{\text{in}} = Ri + L(\theta, i)\frac{\mathrm{d}i}{\mathrm{d}t} + i\omega_{\text{m}}\frac{\mathrm{d}L(\theta, i)}{\mathrm{d}t}, \tag{1}$$

where V_{in} is the applied voltage to a phase, R is the resistance per phase, L is the inductance dependent on the rotor position θ and phase current i. The last term on the right hand side of Eq. 1 is the induced emf, which is a function of angular velocity ω_{m}. From Eq. 1 the instantaneous power can be calculated [7]

$$P_{\text{i}} = Ri^2 + \frac{\mathrm{d}\left(\frac{1}{2}L(\theta, i)i^2\right)}{\mathrm{d}t} + \frac{1}{2}i^2\frac{\mathrm{d}L(\theta, i)}{\mathrm{d}t}, \tag{2}$$

which is equal to the sum of the winding resistance losses given by Ri^2, the rate of change of the field energy (the second term) and the air gap power $\left(\frac{1}{2}i^2\frac{\mathrm{d}L(\theta,i)}{\mathrm{d}\theta}\right)$. Also the air gap power is the product of the electromagnetic torque T_{e} and

rotor speed. Hence, the electromagnetic torque produced by the non-saturating SR machine can be given as

$$T_{\mathrm{e}} = \frac{1}{2} i^2 \frac{\mathrm{d}L(\theta, i)}{\mathrm{d}\theta}. \tag{3}$$

The average power output can be calculated as [8]

$$P_{\mathrm{elec,out}} = \frac{N_{\mathrm{s}} N_{\mathrm{r}} V_{\mathrm{in}}^2}{\omega_{\mathrm{m}}} \left(\int_{\theta_{\mathrm{on}}}^{\theta_{\mathrm{comm}}} \frac{(\theta - \theta_{\mathrm{on}})}{L(\theta, i)} \mathrm{d}\theta - \int_{\theta_{\mathrm{comm}}}^{\theta_{\mathrm{off}}} \frac{(\theta_{\mathrm{comm}} - \theta_{\mathrm{on}} - \theta)}{L(\theta, i)} \mathrm{d}\theta \right), \tag{4}$$

where N_{s} and N_{r} are the number of stator and rotor poles. θ_{comm} is the commutation angle.
The total input power in motoring or generating mode is equal to the mechanical and electrical input powers

$$P_{\mathrm{input}} = P_{\mathrm{mech,in}} + P_{\mathrm{elec,in}}, \tag{5}$$

and

$$P_{\mathrm{mech,in}} = T_{\mathrm{e}} \omega_{\mathrm{m}}, \tag{6}$$

where T_{e} is the torque generated at different angle. and the total output power is

$$P_{\mathrm{out}} = P_{\mathrm{input}} - P_{\mathrm{losses}} = P_{\mathrm{elec,out}}, \tag{7}$$

hence the electrical efficiency is calculated

$$\eta = \frac{P_{\mathrm{elec,out}}}{P_{\mathrm{elec,in}}}, \tag{8}$$

$$P_{\mathrm{elec,in}} = V_{\mathrm{in}} I_{\mathrm{in}}, \tag{9}$$

$$P_{\mathrm{elec,out}} = V_{\mathrm{out}} I_{\mathrm{out}}. \tag{10}$$

Output power of each phase used in this work and simulations:

$$P_{\mathrm{elec,out}} = V_{\mathrm{coil}} i - R i^2. \tag{11}$$

III. Results

During the design exploration process the flux linkage versus phase current for different designs were calculated until the highest energy conversion efficiency by the SRG was found. Due to lower input voltage range and SRG stack size the design process has been more challenging compared to large scale SRGs, where the DC-bus voltage is typically available in hundreds of volts. For the selected design the flux linkage values vs phase current is shown in Figure 6 using two methods, a reference FEM model and commercial software called Simcenter MAGNET 2D/3D. The results show that the MAGNET simulations over-estimate the performance of the SRG and this could be due to the fact that the resistance of windings are not considered in the model.

The simulated results show the phase current i, the voltage across the respective phase coils V_{coil}, and the generated torque T for two cases when the individual phase coils are connected in parallel and series at 3000rpm. The results are shown in Figures 7 and 8 for one phase during excitation and generation.

When the individual phase coils are connected in parallel, in each phase, highest current is generated as the total internal resistance reduces in comparison with the case where coils are connected in series. In both cases the current has increased during the generation mode when the torque is negative.

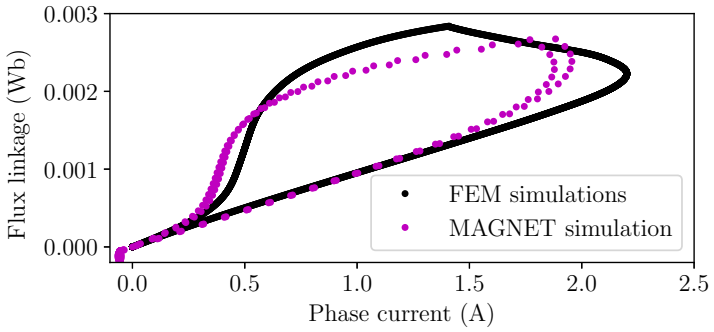

Fig. 6 Simulated flux linkage vs phase current at 3000 rpm for series phase coil configuration.

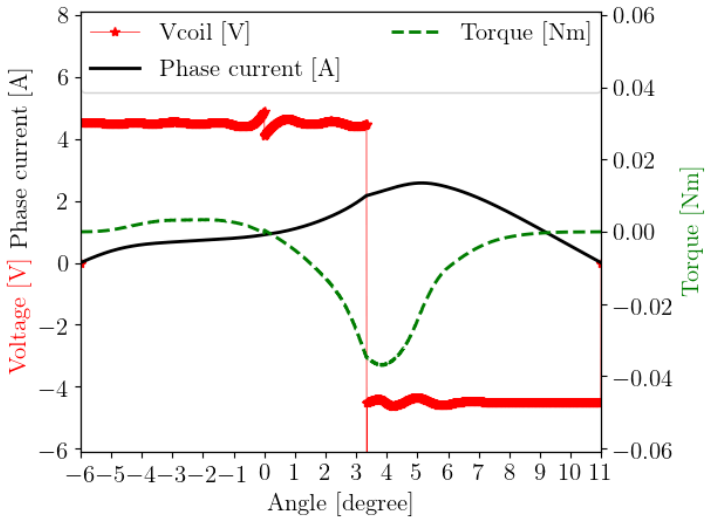

Fig. 7 Simulated voltage and current at one phase and the torque in parallel phase coil configuration. This plot is from the numerical results recorded by simulation (when the rotation speed is 3000 rpm) and should be compared with the experimental results.

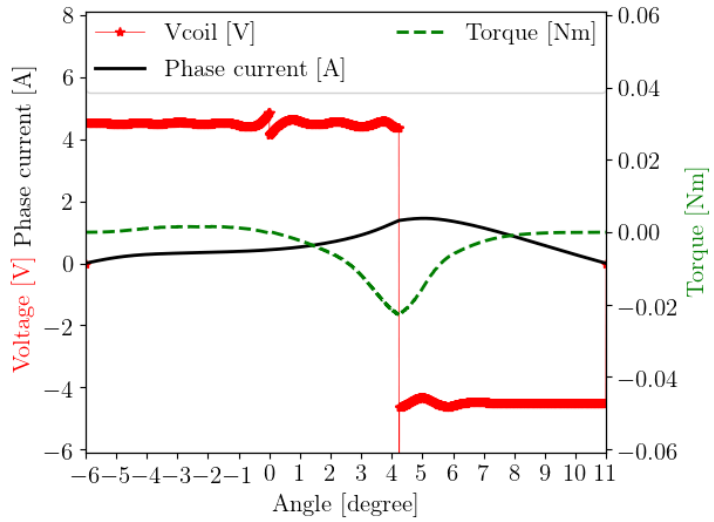

Fig. 8 Simulated voltage and current at one phase and the torque in series phase coil configuration. This plot is from the numerical results recorded by simulation (when the rotation speed is 3000 rpm) and should be compared with the experimental results.

By finding the voltage and current across one phase, the power can be calculated. The power input and output are calculated at different rotational speed corresponding to variation of speed at different aircraft flight phases based on equations shown in the previous section. Figure 9 and 10 show efficiencies and average torque for different rotational speed. As the speed increases, the efficiency of the SRG also increases. For future studies these results will be shown as a function of the flight mission profile.

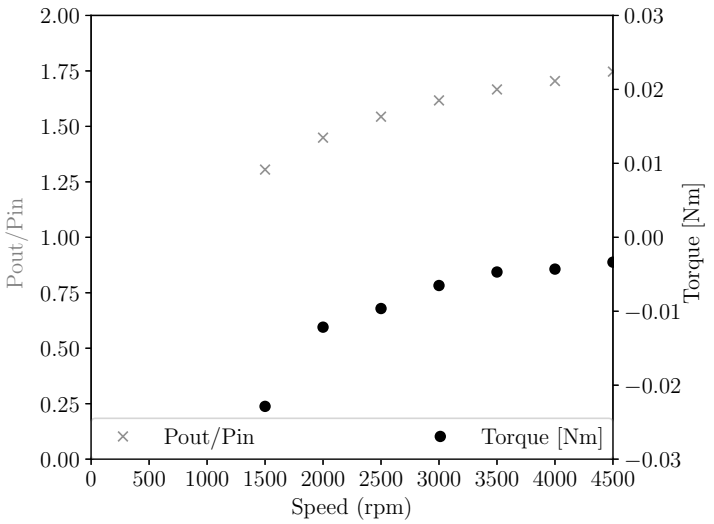

Fig. 9 Simulated average power output over power input by considering the power output and input to one phase and the average torque in parallel phase coil configuration at different speed. The speed range (1500rpm to 4500 rpm) represents the speed at which the shaft will rotate at different points in the flight cycle.

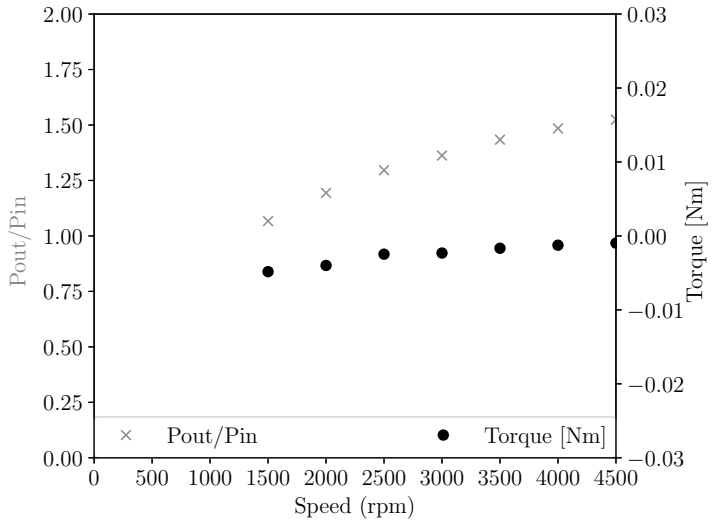

Fig. 10 Simulated average power output over power input by considering the power output and input to one phase and the average torque in series phase coil configuration at different speed. The speed range (1500rpm to 4500 rpm) represents the speed at which the shaft will rotate at different points in the flight cycle.

IV. Conclusion

Self-powered sensing technology is needed to provide in-situ health monitoring for next generation aircraft. In previous studies the use of thermoelectric generators was explored to provide power for sensors and their data processing. As the number of sensors increases, more data needs to be analysed and transmitted wirelessly, more power is needed. In this paper, a switched reluctance generator was designed to be integrated in the engine. The careful selection of topology and switched reluctance excitation and generation timing and control has resulted in achieving high output power to input power ratio. The maximum output power can only be generated if turn on, commutation, and turn off angles are found and applied precisely in actual generator operation. In the case of series phase coil configurations, where the engine was operated at 4500 rpm, the efficiency of greater than 1.6% has been obtained. In the case of parallel phase coil configurations, the efficiency greater than 1.75% has been achieved.

Acknowledgements

This work was supported by the framework of Clean Sky 2 Joint Undertaking through the 82 European Union Horizon 2020 Research and Innovation Programme under Grant I2BS: 717174. We would like to thank Patrick Mirring and Tina Bauer from Schaeffler, and Mathias Gautier and Denis Mouradian from Safran Aircraft Engines for their suggestions in integrating the smart bearing and the SRG to the engine.

References

[1] Zaghari, B., Weddell, A. S., Esmaeili, K., Bashir, I., Harvey, T. J., White, N. M., Mirring, P., and Wang, L., "High Temperature Self-Powered Sensing System for a Smart Bearing in an Aircraft Jet Engine," *IEEE Transactions on Instrumentation and Measurement*, 2020.

[2] White, N. M., and Zaghari, B., "Energy Harvesting: An Overview of Techniques for Use Within the Transport Industry," *IEEE Electrical Insulation Magazine*, Vol. 38, No. 3, 2022, pp. 24–32. https://doi.org/10.1109/MEI.2022.9757916.

[3] Bilgin, B., Howey, B., Callegaro, A. D., Liang, J., Kordic, M., Taylor, J., and Emadi, A., "Making the case for switched reluctance motors for propulsion applications," *IEEE Transactions on Vehicular Technology*, Vol. 69, No. 7, 2020, pp. 7172–7186.

[4] Ferreira, C. A., Jones, S. R., Heglund, W. S., and Jones, W. D., "Detailed design of a 30-kW switched reluctance starter/generator system for a gas turbine engine application," *IEEE Transactions on Industry Applications*, Vol. 31, No. 3, 1995, pp. 553–561.

[5] Valdivia, V., Todd, R., Bryan, F. J., Barrado, A., Lázaro, A., and Forsyth, A. J., "Behavioral modeling of a switched reluctance generator for aircraft power systems," *IEEE Transactions on Industrial Electronics*, Vol. 61, No. 6, 2013, pp. 2690–2699.

[6] Zaghari, B., Stuikys, A., Weddell, A. S., and Beeby, S., "Efficient Energy Conversion in Electrically Assisted Bicycles Using a Switched Reluctance Machine Under Torque Control," *IEEE Access*, Vol. 8, 2020, pp. 202401–202411. https://doi.org/10.1109/ACCESS.2020.3036373.

[7] Krishnan, R., *Switched reluctance motor drives: modeling, simulation, analysis, design, and applications*, CRC press, 2017.

[8] Asadi, P., "Development and application of an advanced switched reluctance generator drive," Ph.D. thesis, Texas A & M University, 2010.